INSTABILITY DYNAMICS WITH ELECTRON CLOUD BUILDUP IN LONG BUNCHES*

M. Blaskiewicz†, BNL 911B, Upton, NY 11973-5000, USA

Abstract

For long bunches, trailing edge multi-pacting causes the electron cloud density at the trailing edge of the bunch to be significantly larger than the cloud density during the early and central portions of the bunch. The effective wakefield is modeled and compared with hand estimates. Instabilty simulations, which include the effect of nonlinear space charge, are described.

INTRODUCTION

Fast electron cloud instabilities have been obvserved in the Los Alamos PSR [1, 2, 3, 4, 5, 6] and may be problematic for the Oak Ridge SNS [5, 6]. For both these machines the transverse electron oscillation period is much less than the bunch length. The electron motion is nearly adiabatic and the electron density can strongly increase as the tail of the bunch passes. This is illustrated in Fig. 1, which shows CSEC [6] simulation results for the PSR. The secondary emission parameters of the stainless steel wall agree well with the model in [7]. It is likely that significant wall conditioning would be needed before the PSR could reach a bunch intensity of 8 μC, but the author knows of no detailed data under such conditions and it seemed more reasonable to adopt a well defined state. In any case, the purpose of the present paper is to describe computational techniques.

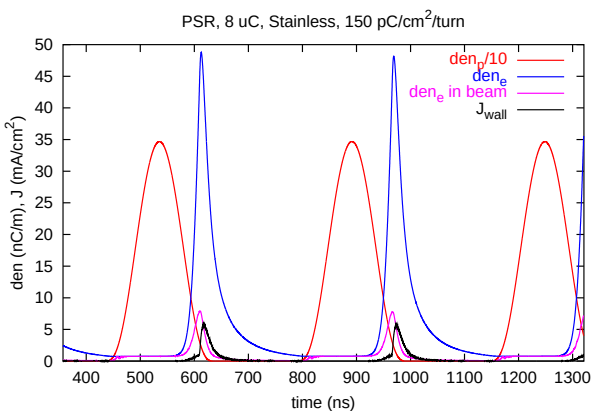

Figure 1: CSEC simulations for a high intensity PSR with an unscrubbed stainless steel beam pipe.

* Work supported by U.S. D.O.E. under contracts DE-AC05-00OR2275 and DE-AC02-98CH10886.

† blaskiewicz@bnl.gov

ELECTRON CLOUD WAKEFIELDS

Consider a proton bunch with line density λ_p and radius a_p, interacting with an electron cloud with line density $-\lambda_e$ and radius a_e. Assume both clouds have uniform density and are centered horizontally with $x = 0$. Let y_e and y_p be the vertical offsets of the electron and proton centroids, respectively. Then, the net force per unit length on the protons is

$$F_p = \frac{\lambda_p \lambda_e}{2\pi\epsilon_0 \max(a_p^2, a_e^2)}(y_e - y_p), \quad (1)$$

$$= \frac{\lambda_p \lambda_{e,i}}{2\pi\epsilon_0 a_p^2}(y_e - y_p), \quad (2)$$

$$= -F_e, \quad (3)$$

where $-\lambda_{e,i}$ is the line charge density of electrons within the beam and F_e is the net force per unit length on the electrons.

The electrons have small longitudinal velocities, so consider a single longitudinal slice. Define the time dependent electron bounce frequency

$$\omega_e^2(t) = \frac{e\lambda_p(t)}{2\pi\epsilon_0 m_e a_p^2},$$

where $I_p(t) = \beta c \lambda_p(t)$ is the instantaneous proton current through the slice. The equation of motion for the electron centroid is

$$\frac{d^2 y_e}{dt^2} = \omega_e^2(t)[y_p(t) - y_e]. \quad (4)$$

The average electric field on the protons due to the electrons is

$$E_e(t) = F_p/\lambda_p = \frac{\lambda_{e,i}(t)}{2\pi\epsilon_0 a_p^2}(y_e - y_p). \quad (5)$$

Equation (5) will be referred to as the "full" model of the electron force. The "central" model of the force corresponds to replacing $\lambda_{e,i}(t)$ with the the value of $\lambda_{e,i}$ in the center of the bunch. The central model neglects the flash on the tail.

There are several approximations involved in the derivation of equation (5) and it is prudent to check its accuracy. Toward this end CSEC was modified to allow for a nearly cylindrically symmetric electron cloud (NCSEC). The proton beam was taken to be round, but with a time dependent vertical offset, $y_p(t)$. Within the round beam pipe of radius b the electric field due to the protons is

$$\mathbf{E}_p(t) = \frac{\lambda_p(t)}{2\pi\epsilon_0}\left[\mathbf{G}_0(x, y - y_p) - \frac{(xy_p^2, yy_p^2 - b^2 y_p)}{x^2 y_p^2 + (yy_p - b)^2}\right]. \quad (6)$$

The code allows for uniform proton density profiles with $\mathbf{G}_0(x,y) = (x,y)/\max(a_p^2, x^2+y^2)$, and smooth proton profiles with $\mathbf{G}_0(x,y) = (x,y)/(a_p^2+x^2+y^2)$.

It is assumed that y_p is small enough so that the electron density can be approximated at each time step as

$$\rho_e(x,y) = \rho_0(r,t) + \rho_1(r,t)\cos(\theta), \tag{7}$$

where $r^2 = x^2+y^2$ and $\theta = 0$ for a particle on the positive y axis. The particles were binned onto a radial grid with $M \sim 200$ mesh points. Define the triangle function

$$T(x) = \begin{cases} 1-|x|, & |x|<1 \\ 0, & 1 \le |x| \end{cases} . \tag{8}$$

The first step was to loop over the N electron macroparticles interpolating onto the radial grid. This produced the arrays

$$\Lambda_0(m) = \sum_{k=0}^{N} q_k T(m - M r_k/b)$$

and

$$\Lambda_1(m) = \sum_{k=0}^{N} q_k y_k T(m - M r_k/b),$$

where q_k is the charge per unit length of the kth electron macro particle. The force due to $\Lambda_0(m)$ is the same as for CSEC. For $\Lambda_1(m)$ the potential due to the electrons is given by

$$\Phi_e(x,y) = \sum_m \frac{\Lambda_1(m)}{2\pi\epsilon_0}\left(\frac{y}{\max(r^2, r_m^2)} - \frac{y}{b^2}\right) \tag{9}$$

where $r_m = mb/M$. The wake force on the protons was obtained by averaging $-\nabla\Phi_e = \mathbf{E}_e(x,y)$ over a disk of radius a_p. NCSEC results for a uniform density beam are shown in Figures 2 through 4. Corresponding figures for a smooth distribution are shown in figures 5 through 7.

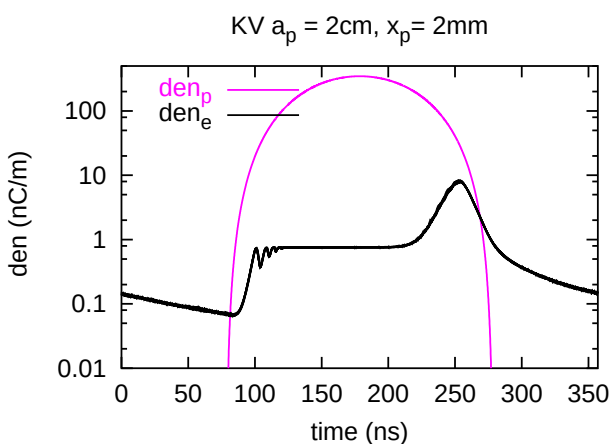

Figure 2: proton and electron line density within a uniform beam for 9 turns of PSR. The proton beam had a 2cm radius and uniform transverse density.

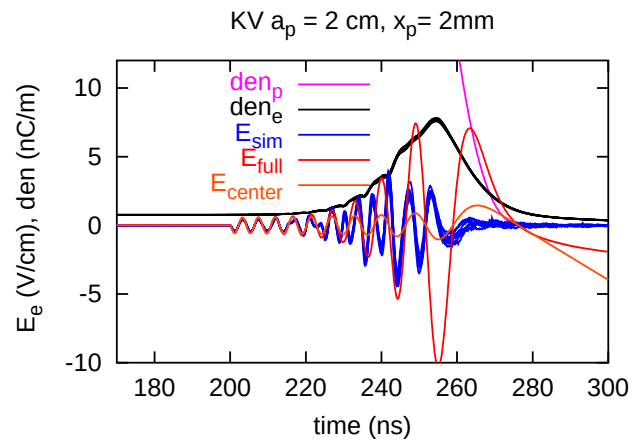

Figure 3: NCSEC simulations for PSR. The proton bunch was offset by 2mm for 0.5ns starting at 200ns. Values of $\lambda_p = den_p$ and $\lambda_{e,i} = den_e$ for 9 turns are shown. Also shown are the average transverse field from the simulations and the two analytic models.

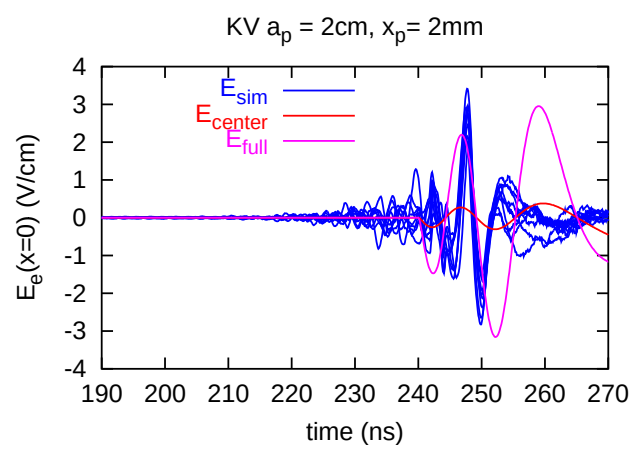

Figure 4: NCSEC simulations for PSR. The proton bunch was offset by 2mm for 0.5ns starting at 240ns.

First consider the uniform tranverse profile. The densities for 9 consectutive turns are overplotted in Figure 2. This gives an indication of the statistical accuracy. Figure 3 shows the line densities as well as the simulated wakefields and the two models. The electron oscillation was started by offsetting the proton beam by 2mm for 0.5 nanoseconds starting at 200ns. The simulation results lie somewhere between the full and central models. Figure 4 shows results when the offset begins at 240 ns.

Next consider Figures 5 through 7. The value of $a_p = 1.2$ cm was chosen so that the potential difference between the center of the pipe and the pipe wall were the same for the two cases. The electron densities shown in figure 5 are close to those in Figure 2, but the wakefields are quite different. Figure 6 shows only the central model since even it overestimates the wakefield. Both the models are shown in Figure 7 but the central model is no worse than the full

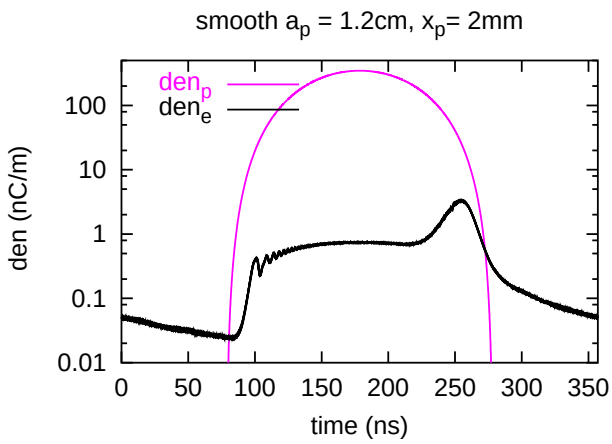

Figure 5: proton and electron line density within the beam for 9 turns of PSR. The transverse proton beam density scaled as $(1 + (r/1.2\ \mathrm{cm})^2)^{-4}$.

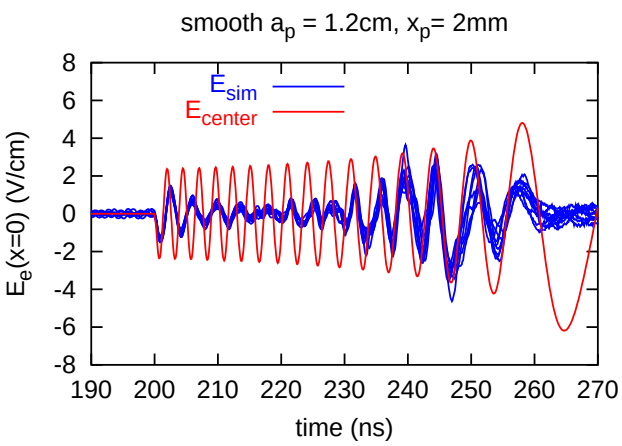

Figure 6: NCSEC simulations for PSR corresponding to Figure 5. The proton bunch was offset by 2mm for 0.5ns starting at 200ns. The average transverse field from the simulations and the central analytic model are shown.

model. In the actual PSR the beam has a smooth transverse profile so Figures 5 through 7 show the appropriate regime.

The simulations shown in Figures 2 through 7 took about 10 minutes per turn for a single electron cloud slice. For an instability simulation one needs to apply electron cloud kicks about 10 times per betatron period to accurately model the detuning with betatron amplitude, and at least 100 periods need to be modeled to see the instability. It is not clear whether the noise levels in Figures 4 and 7 are sufficently low to remove spurious growth. With these things in mind the author chose to adopt a simple wakefield model for instability simulations. The central model appears to fit the PSR best, and this model will be used for the rest of the note.

The timelike variable for the protons is azimuth $\theta = s/R$, where s is the longitudinal Serret-Frenet coordinate and R is the average radius of the accelerator. The time-

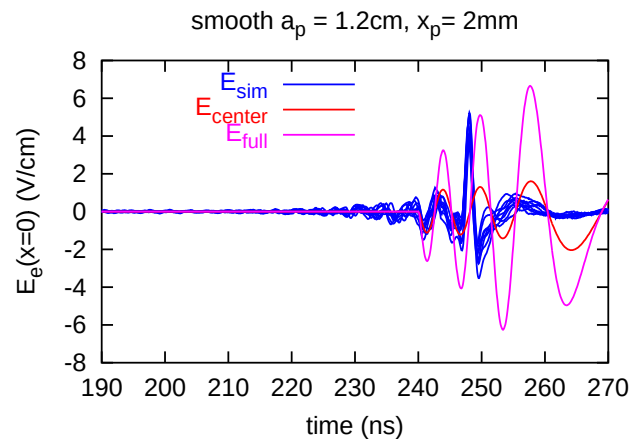

Figure 7: NCSEC simulations for PSR corresponding to Figure 5. The proton bunch was offset by 2mm for 0.5ns starting at 240ns. The average transverse field from the simulations and the two analytic models are shown.

like coordinate for the electrons is time as measured in the lab frame t. The electron cloud will be approximated by slices, and the θ coordinates of the slices are uniformly spaced around the ring. The lattice functions for the proton beam, and hence the beams transverse dimensions, vary with azimuth. Many slices would be required to faithfully model the variation in electron bounce frequency due to the beam size variations. Instead, a damping factor will be introduced into the electron equation of motion.

$$\frac{d^2 y_e}{dt^2} = \omega_e^2(t)[y_p(t) - y_e] - \frac{\omega_e(t)}{Q_e}\frac{dy_e}{dt}. \qquad (10)$$

For the PSR and SNS one finds $Q_e \approx 3$.

SPACE CHARGE AND OTHER DYNAMICAL CONCERNS

With equation (10) and assuming uniform focusing the vertical equation of motion for the protons is

$$\frac{d^2 y_p}{d\theta^2} = -Q_y^2 y_p + Q_p^2(y_e - y_p) + F_{sc,y}(x, y, \theta, t), \quad (11)$$

where Q_y is the vertical tune (chromaticity is easy to include),

$$Q_p^2 = \frac{e\lambda_{e,i}}{2\pi\epsilon_0\omega_0^2\gamma m_p a_p^2}$$

measures the strength of the electron cloud, and $F_{sc,y}$ is the vertical component of the space charge force. For horizontal motion the term proportional to Q_p^2 is absent. Previous work [6, 8] assumed that the space charge force was linear in the transverse offset. The PSR has a smooth transverse profile so some variation in space charge tune shift with betatron amplitude is present. One option is to do a full solution of the two dimensional Poisson equation [9, 10]

with many longitudinal slices along the bunch. This appears to be computationally difficult and the author is not aware of any, published, bunched beam simulations using this approach. A simpler model will be adopted.

Let the particles cross the reference azimuth with offsets x_k and y_k at times t_k. The direct space charge kick at coordinates x, y, t is approximated as

$$\mathbf{F}_{sc}(x,y,t) = (\partial_x, \partial_y) \sum_m U(x - x_m, y - y_m, t - t_m), \tag{12}$$

where the two particle Green's function is

$$U(x,y,t) = S(t)\cos(kx)\cos(ky)/k^2. \tag{13}$$

The parameter k controls the nonlinearity of the space charge force and $S(t)$ controls the size and longitudinal smoothing length of the space charge force. The first step in the algorithm is to generate a uniform mesh in t. The mesh spacing, Δt, is around ten times smaller than the smoothing applied later. Next generate the four arrays

$$S_{cc}(n) = \sum_m \cos(kx_m)\cos(ky_m)T(n - t_m/\Delta t),$$

$$S_{cs}(n) = \sum_m \cos(kx_m)\sin(ky_m)T(n - t_m/\Delta t),$$

$$S_{sc}(n) = \sum_m \sin(kx_m)\cos(ky_m)T(n - t_m/\Delta t),$$

$$S_{ss}(n) = \sum_m \sin(kx_m)\sin(ky_m)T(n - t_m/\Delta t).$$

Each of these arrays is smoothed using two applications of a convolution with $\exp(-4|t|/\tau_s)$, where τ_s is the equivalent length of the final smoothing function. This is done using an algorithm whose operation count scales linearly with the number of mesh points. Finally, the sum rules for sinusoids is used to apply the force in an algorithm that scales linearly with the number of macro particles. The transverse single particle dynamics is handled using matricies where the phase advance can be a function of the betatron amplitude (octupolar detuning) and the momentum offset (chromaticity). The longitudinal motion is updated using a linearized RF force. Nonlinear RF has been included but no runs produced any qualitative effects for the PSR parameter regime.

To obtain the initial coordinates one defines a longitudinal dimension N_ℓ. Next create the set of order pairs of half integers

$$\{(m+1/2, n+1/2) : (m+1/2)^2 + (n+1/2)^2 \le N_\ell^2\}.$$

This is a uniformly spaced set of lattice points on the plane which lie within a circle of radius N_ℓ. An ordering is imposed (actually assigned during creation) and the normalized coordinates $\mathbf{x} = (m+1/2, n+1/2)/N_\ell$ are generated. A smooth longitudinal profile is obtained by the mapping

$$(\tau, \dot{\tau}/\omega_s) = \tau_b \frac{\mathbf{x}}{2|\mathbf{x}|}\sqrt{1 - (1 - |\mathbf{x}|^2)^{1/(\mu+1)}}, \tag{14}$$

so that the line density is proportional to

$$(1 - 4t^2/\tau_b^2)^{\mu+1/2}.$$

While this assignment limits the possible longitudinal profiles, is greatly suppresses startup fluctuations.

To generate transverse coordinates start by finding four uniform deviates within the unit 4-sphere, $\mathbf{x} = (r_1, r_2, r_3, r_4)$. Normalized betatron coordinates are obtained using (14) with $\mu = 2$ and τ_b replace by $2a_p$. In terms of the two transverse actions J_x and J_y, with $0 < J_x$, $0 < J_y$, and $J_x + J_y < 1$; the Vlasov density is

$$\begin{aligned} F(J_x, J_y) &\propto \frac{1 - (1 - J_x - J_y)^3}{J_x + J_y}(1 - J_x - J_y)^2 \\ &\approx 3(1 - J_x - J_y)^3. \end{aligned}$$

The two dimensional charge density is smooth and fairly well approximated by $(a_p^2 - x^2 - y^2)^4$, with $x^2 + y^2 < a_p^2$.

PRELIMINARY RESULTS

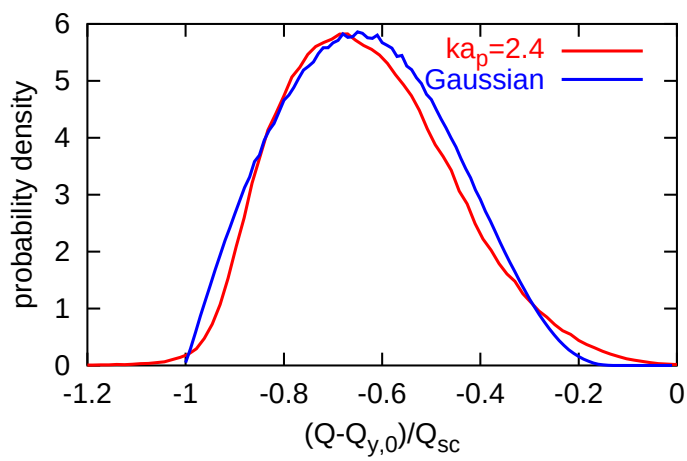

Figure 8: Normalized tune distributions from the simulations and for a round Gaussian beam. The Gaussian results were obtained using first order pertubation theory with the integrals computed numerically.

Figure 8 showns the normalized space charge tune shift distribution with $ka_p = 2.4$ for a rectangular bunch ($\mu = -1/2$), and compares it with the results for a round Gaussian beam with the exact Coulomb force. When viewed in this way the distributions are fairly similar and the value $k = 2.4/a_p$ will be adopted. Figure 9 shows a scatter plot of vertical tune versus longitudinal position for the PSR. The peak tune shift is somewhat larger than has been reported previously [11], but is not absurd. Figure 10 shows a scatter plot of the vertical position along the bunch for the PSR just beyond threshold, after 1000 turns. Figure 11 shows the evolution of the coherent action for the same parameters. Also shown are simulations using linear space charge with the same average tune shift, and results with direct space charge turned off. Space charge destabilizes

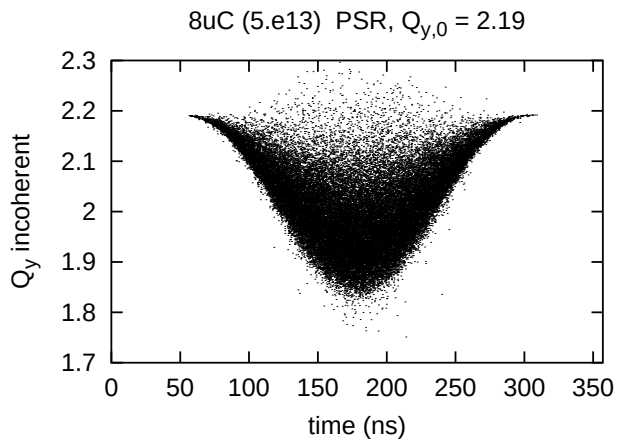

Figure 9: Scatter plot of betatron tune with longitudinal position from the simulations.

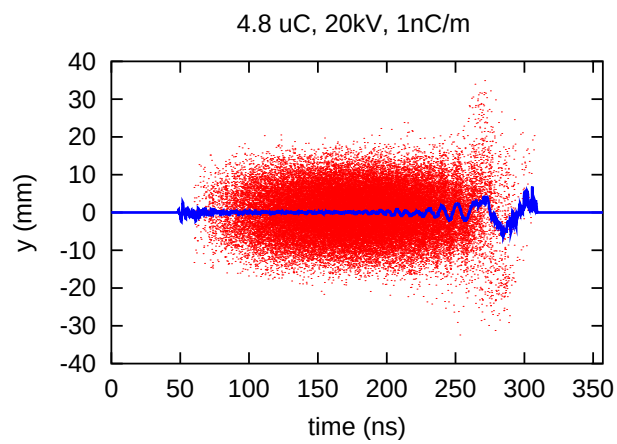

Figure 10: Scatter plot of vertical versus longitudinal position for a PSR beam just beyond threshold current and evolved over 1000 turns.

the beam and nonlinear space charge is less destabilizing than linear space charge.

Simulations for various parameters are shown in Figure 12. Notice that that the red trace corresponds to 3×10^{13} protons and the pink trace to 5×10^{13} protons for the same bunch length. The electron density is only 20% higher for the case with 3×10^{13}. Clearly, the value of the electron density is critical for estimating the threshold. Figure 13 shows the corresponding situation for half the number of protons and half the RF voltage with the same electron densities. Notice that Figure 13 shows half the turns of Figure 12. Halving the number of protons and the RF voltage while keeping the number of electrons constant, destabilizes the beam. Figure 14 shows threshold data for the PSR. Unless there is a serious error in the simulations, the linear scaling of threshold voltage with beam intensity is a coincidence. That is to say, the electron cloud density must vary appropriately with intensity to obtain a linear scaling. The weak dependence on bunch length also appears to depend on the details of the electron cloud.

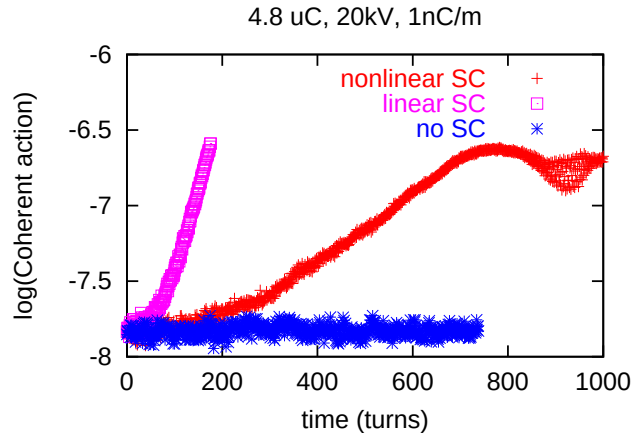

Figure 11: Evolution of the coherent action for a beam just beyond threshold with nonlinear space charge (red). A simulation with linear space charge and the same average tune shift (violet) shows a strong instability, while neglecting space charge (blue) yields a stable beam.

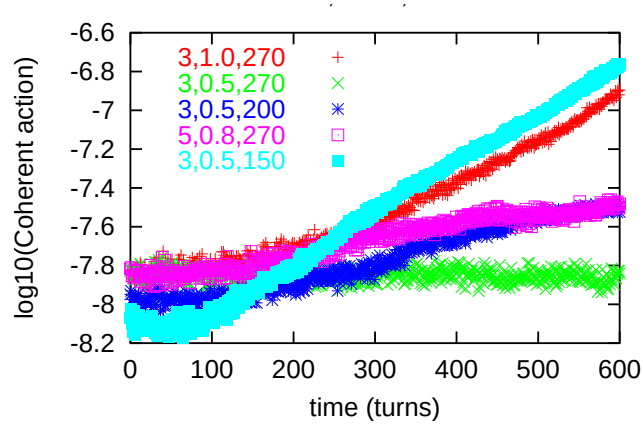

Figure 12: Simulations for various values of $N_p(10^{13})$, λ_e (nC/m) and τ_b (ns). All the simulations assumed a 20 kV RF voltage.

CONCLUSIONS

The effect of the electron burst from single pass multipacting on the electron cloud wakefield has been studied. For beams with a uniform transverse density the actual wakefield was between the predictions of two simple models. For beams with a smooth transverse density the central model, which assumed a constant electron line density, produced the best approximation. The PSR corresponds to the second case. A simple simulation technique to include the dependence of space charge tune shift on betatron amplitude was introduced. The free parameter k was chosen so that the tune distribution for the model agreed fairly well with the tune distribution for a round Gaussian beam. Instability simulations for PSR showed that nonlinear space charge was less destabilizing than linear space charge. Neglecting space charge entirely produced the most stable simulations.

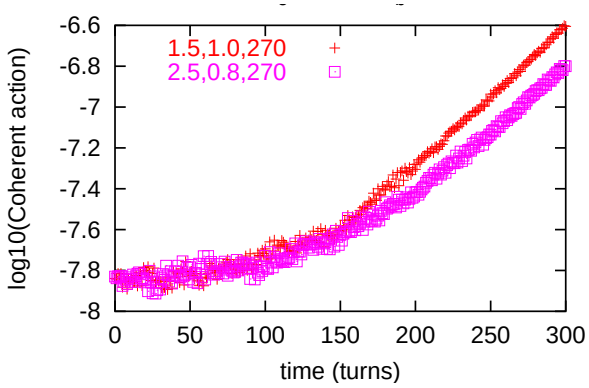

Figure 13: Simulations for various values of $N_p(10^{13})$, λ_e $(\mathrm{nC/m})$ and τ_b (ns). Both the simulations assumed a 10 kV RF voltage.

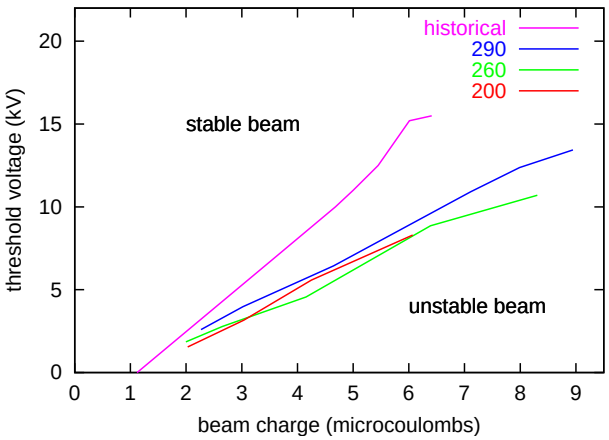

Figure 14: Reproduced from [6](Courtesy R.J. Macek). Threshold RF voltage versus beam intensity. The threshold RF voltage is the smallest RF voltage for which the beam is stable. The historical curve represents the situation before the direct H^- upgrade and the extended run of 2001. Threshold curves near the end of the 2001 run for injected bunch lengths of 200, 260, and 290 ns are shown.

REFERENCES

[1] D. Neuffer *et. al. NIM* **A321** p1 (1992).

[2] M. Plum, PSR Tech Note PSR-94-001 (1994).

[3] M. A. Plum *et. al* PAC97 p 1611.

[4] R. Macek, AIP Conf. 448, p116, (1998)

[5] V. Danilov *et.al* PAC99 TUA 52.

[6] M. Blaskiewicz, M. A. Furman, M. Pivi, R. J. Macek *Phys. Rev. ST Accel. Beams* **6**, 014203 (2003).

[7] M. A. Furman, M. T. F. Pivi *Phys. Rev. ST Accel. Beams* **5** 124404 (2002).

[8] M. Blaskiewicz, *Phys Rev S.T Accel Beams* **1** 044201 (1998).

[9] H. Qin, R. C. Davidson, E. Startsev, W. W. Lee, PAC01, 693, (2001)

[10] H. Qin, E. Startsev, R. C. Davidson *Phys. Rev. ST Accel. Beams* **6** 014401 (2003).

[11] S. Cousineau, J. A. Holmes, J. Galambos, A. Fedotov, J. Wei, R. Macek *Phys. Rev. ST Accel. Beams* **6** 074202 (2003).